


# Materials Integrating Photochemical Upconversion

Catherine E. McCusker<sup>1</sup> · Felix N. Castellano<sup>1</sup> 

Received: 11 January 2016 / Accepted: 14 March 2016 / Published online: 29 March 2016  
© Springer International Publishing Switzerland 2016

**Abstract** This review features recent experimental work focused on the preparation and characterization of materials that integrate photochemical upconversion derived from sensitized triplet–triplet annihilation, resulting in the conversion of low energy photons to higher energy light, thereby enabling numerous wavelength-shifting applications. Recent topical developments in upconversion include encapsulating or rigidifying fluid solutions to give them mechanical strength, adapting inert host materials to enable upconversion, and using photoactive materials that incorporate the sensitizer and/or the acceptor. The driving force behind translating photochemical upconversion from solution into hard and soft materials is the incorporation of upconversion into devices and other applications. At present, some of the most promising applications of upconversion materials include imaging and fluorescence microscopy, photoelectrochemical devices, water disinfection, and solar cell enhancement.

**Keywords** Photochemical upconversion · Triplet–triplet Annihilation · Wavelength shifting · Light emitting materials · Solid state upconversion · Soft photonic materials

---

This article is part of the Topical Collection “Photoluminescent Materials and Electroluminescent Devices”; edited by Nicola Armaroli, Henk Bolink; please follow CAP workflow

---

✉ Felix N. Castellano  
fncastel@ncsu.edu

<sup>1</sup> Department of Chemistry, North Carolina State University, Raleigh, NC 27695-8204, USA

# 1 Introduction to Photochemical Upconversion

## 1.1 Introduction

Photon upconversion afforded via sensitized triplet–triplet annihilation (TTA) is a regenerative photochemical process resulting in the net frequency upconversion of light. Sensitized TTA and photon upconversion, first introduced by Parker and Hatchard in the early 1960s, incorporated the exclusive use of organic sensitizers and acceptors [1–3]. By selectively exciting the sensitizer chromophore, these authors were able to observe blue-shifted emission (fluorescence) characteristic of the acceptor chromophore, concomitant with nonlinear excitation light power dependence. They concluded this upconverted emission was due to the interaction of two excited triplet acceptors, which resulted in one excited singlet acceptor and one ground state acceptor. These initial systems suffered from low efficiency and further advancement in this field was not to be realized for several decades. During the last 13 years there has been a resurgence of interest in the field of sensitized photon upconversion prompted by the change to inorganic (transition metal containing) sensitizers featuring unity to near quantitative intersystem crossing (ISC) yields [4–6]. Much of this initial work has been developed in fluid solution, where the sensitizer and acceptor can diffuse freely. With few exceptions, it has been during the last 8 years that upconversion in numerous host materials and media has made significant progress.

The process of photon upconversion is displayed pictorially in Fig. 1. Sensitizer molecules absorb light and are promoted into a singlet excited state, which intersystem crosses into a triplet excited state. When the triplet sensitizer encounters an acceptor it can undergo a Dexter-type collisional triplet–triplet energy transfer (TTET), forming the triplet excited state of the acceptor. When two triplet acceptors meet they can engage in TTA (essentially a second TTET step), resulting in one excited singlet acceptor and one ground state acceptor. The excited singlet acceptor can then fluoresce, returning to the ground state by the emission of this higher

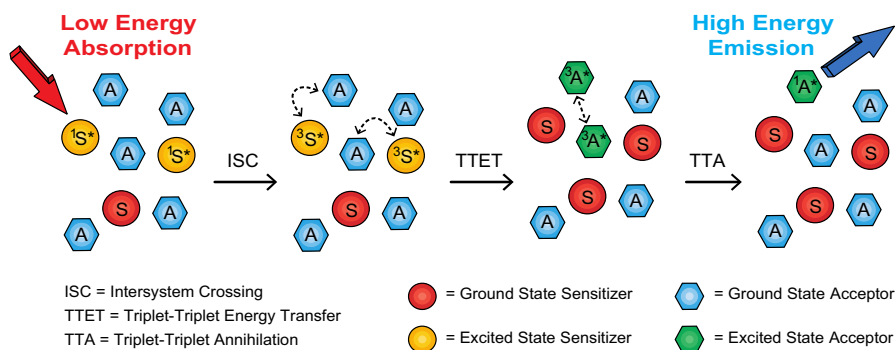


**Fig. 1** Pictorial illustration of sensitized photon upconversion. The orange circles are ground state sensitizers, the yellow circles are excited state sensitizers, the blue hexagons are ground state acceptors, and the green hexagons are excited state acceptors

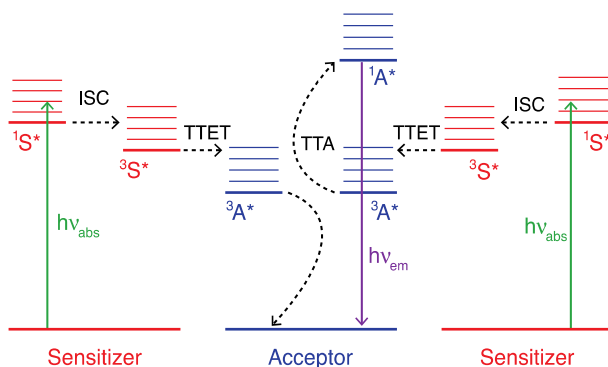


**Fig. 2** Qualitative Jablonski diagram illustrating the relative energy levels of sensitizer and acceptor required for photochemical upconversion

energy photon. The relative energetics of these states is important to realize successful photon upconversion. The Jablonski diagram in Fig. 2 presents the energies of the relevant states. Most important is that the sum of the energy of two triplet acceptors must be greater than or equal to the energy of the resultant excited singlet state ( ${}^3A^* + {}^3A^* \geq {}^1A^*$ ) otherwise the annihilation reaction cannot produce sufficient energy to form the emitter singlet state. For favorable (exothermic) energy transfer, the acceptor triplet state must be lower in energy than the sensitizer triplet state, and for true upconversion (i.e., the acceptor emission is located at a higher frequency with respect to the sensitizer absorption) the acceptor singlet state must be higher in energy than the sensitizer singlet state. To meet these requirements, the acceptor should have a large singlet–triplet gap and the sensitizer should have a small singlet–triplet gap. Given these energetic criteria, the acceptor is generally possesses  $\pi$ - $\pi^*$  excited states with large values of  $2J$ .

## 1.2 Quantifying Photon Upconversion

As illustrated in Fig. 2, two absorbed photons are required for every one emitted photon, implying that the maximum yield for this process is 50 % based on absorbed photons. As a result, the upconverted emission does not have a simple linear dependence on light intensity [7]. The concentration of triplet acceptors, and therefore, the intensity of the upconverted fluorescence, is a function of two competing rates (Eq. 1), where  $k_T$  is the intrinsic first order and pseudo-first order decay pathways for  ${}^3A^*$  and  $k_{TT}$  is the second order TTA rate constant.

$$\frac{d[{}^3A^*]_t}{dt} = -k_T[{}^3A^*] - k_{TT}[{}^3A^*]_t^2 \quad (1)$$

In the weak annihilation limit,  $k_T$  is much larger than  $k_{TT}[{}^3A^*]$ , and first order decay to the ground state is the dominant relaxation pathway for  ${}^3A^*$ . In this limit, the upconverted emission intensity can be expressed as shown in Eq. 2 where  $N_F$  is

the upconverted fluorescence intensity and  $\Phi_F$  is the fluorescence quantum yield of the acceptor.

$$N_F = \frac{\phi_F k_{TT} [{}^3A^*]_0^2}{2k_T} \quad (2)$$

In this limit,  $N_F$  is proportional to  $[{}^3A^*]^2$ , which means it has a quadratic dependence on excitation light intensity, i.e., proportional to the square of the triplet acceptor population. In the strong annihilation limit,  $k_{TT}[{}^3A^*]$  is much larger than  $k_T$  and TTA becomes the dominant relaxation pathway for  ${}^3A^*$ . In this limit, the upconverted emission intensity can be expressed as Eq. 3, where  $N_F$  is proportional to  $[{}^3A^*]$ , and therefore, has a linear dependence on excitation light intensity.

$$N_F = \phi_F [{}^3A^*]_0 \quad (3)$$

The strong annihilation limit is where the efficiency of TTA becomes maximized, and therefore, in any application it is desirable for the device or process to operate under these conditions. Therefore, the system will favor the strong annihilation limit if one minimizes  $k_T$  and maximizes  $k_{TT}[{}^3A^*]$ . The intrinsic decay rate of  ${}^3A^*$  cannot be changed, but also included in the  $k_T$  term is the pseudo-first order quenching of  ${}^3A^*$  by trace dissolved oxygen. Complete exclusion of oxygen from the system is the best way to minimize  $k_T$ . Assuming that TTET quenching has already reached saturation, maximizing  $k_{TT}[{}^3A^*]$  is afforded by increasing the concentration of  ${}^3A^*$ , either by increasing the absorbance of the sensitizer or the intensity of the excitation light.

The power dependence of the upconverted emission signal is one metric that is used to judge the performance of an upconversion composition. When the

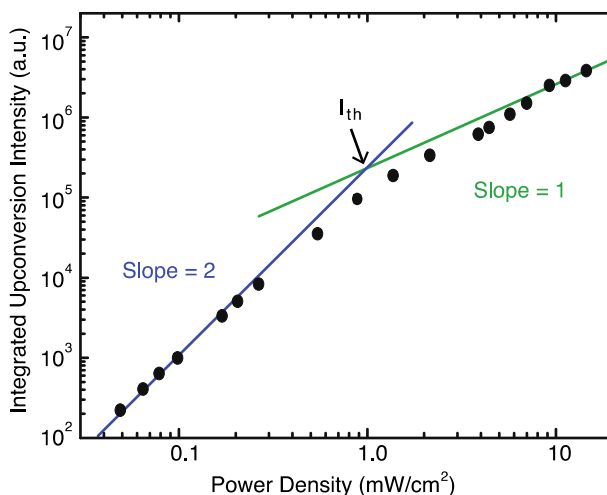


**Fig. 3** Representative example of the incident light power dependence on upconverted emission intensity, plotted on a logarithmic scale

upconverted emission intensity of a system is plotted vs. incident excitation power density on a logarithmic scale, as shown in Fig. 3, regions that are in the weak annihilation limit will have a slope of 2, regions in the strong annihilation limit will have a slope of 1, and intermediate regions, where  $k_T \approx k_{TT}[^3A^*]$ , will have slopes varying between 2 and 1 depending upon their relative proportions. The threshold intensity ( $I_{th}$ ) is the crossover point between the weak annihilation limit and the strong annihilation limit, defined as the crossing point between the slope = 1 line and the slope = 2 line on a logarithmic scale. A system or device has to operate above this threshold power density to reach the maximum upconversion efficiency possible for the given composition.

Upconversion quantum yield ( $\Phi_{UC}$ ) is another useful metric to evaluate upconversion systems. Conceptually,  $\Phi_{UC}$  is the product of the yields of all the steps involved in the upconversion process, as shown in Eq. 4 where  $\Phi_{ISC}$  is the intersystem crossing yield in the sensitizer,  $\Phi_{TTET}$  is the triplet–triplet energy transfer yield,  $\Phi_{TTA}$  is the triplet–triplet annihilation yield, and  $\Phi_F$  is the fluorescence quantum yield of the acceptor.

$$\phi_{UC} = \phi_{ISC} \times \phi_{TTET} \times \phi_{TTA} \times \phi_F \quad (4)$$

Practically, the upconversion quantum yield is often measured relative to a known standard using Eqs. 5 [6] or 6 [8] where  $\Phi_{std}$  is the quantum yield of the standard,  $A$  is the absorbance of the standard or upconversion sample,  $I$  is the integrated emission intensity of the standard and upconversion samples, and  $\eta$  is the refractive index of the medium. The factor of two is included to scale the maximum  $\Phi_{UC}$  to 1 rather than 0.5.

$$\phi_{UC} = 2\phi_{std} \left( \frac{A_{std}}{A_{UC}} \right) \left( \frac{I_{UC}}{I_{std}} \right) \left( \frac{\eta_{UC}}{\eta_{std}} \right)^2 \quad (5)$$

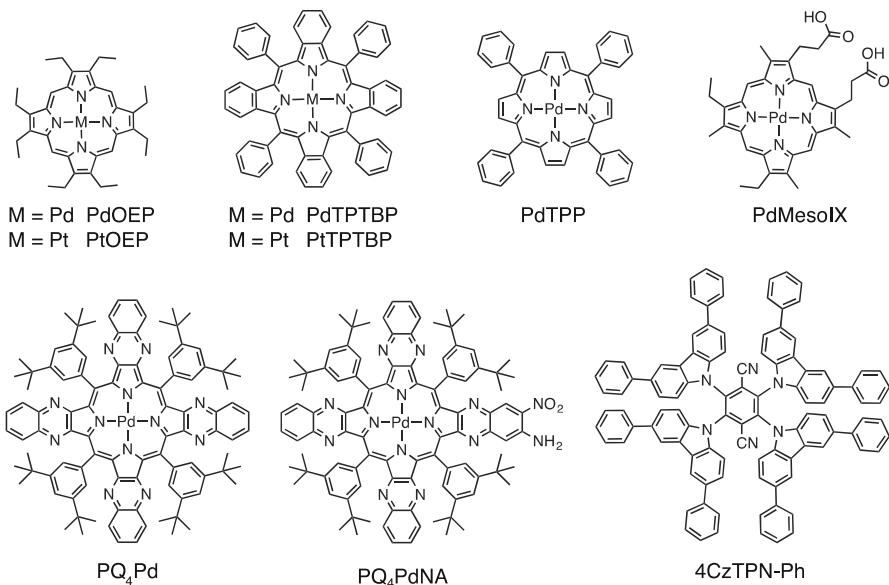
$$\phi_{UC} = 2\phi_{std} \left( \frac{1 - 10^{-A_{std}}}{1 - 10^{-A_{UC}}} \right) \left( \frac{I_{UC}}{I_{std}} \right) \left( \frac{\eta_{UC}}{\eta_{std}} \right)^2 \quad (6)$$

Under optically dilute conditions ( $A \leq 0.1$ ) the simplified Eq. 5 can be used, and under more concentrated conditions the expanded Eq. 6, where  $1 - 10^{-A}$  is the fraction of light absorbed by the sample, must be used. The challenge of this approach, especially for non-solution measurements, is choosing an appropriate, well-established quantum yield standard. An alternative to using a separate quantum yield standard is to use the prompt fluorescence of the acceptor as an internal standard. This method, developed by Schmidt and co-workers [9], uses pulsed laser excitation to directly measure  $\Phi_{TTA}$  (Eq. 7).

$$\phi_{TTA} = \frac{2F_d E_p \lambda_d}{F_p E_d \lambda_p} \quad (7)$$

In this model, the upconverting sample is excited at two different excitation wavelengths, one that will exclusively excite the sensitizer and generate delayed fluorescence ( $\lambda_d$ ) and one that will exclusively excite the acceptor and generate

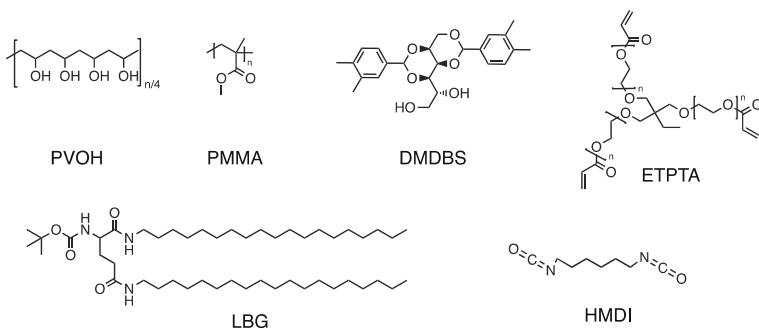
prompt fluorescence ( $\lambda_p$ ). The integrated emission intensity of the prompt fluorescence ( $F_p$ ) is then compared to the integrated intensity of the total upconverted emission ( $F_d$ ). This model assumes that all of the laser pulse energy ( $E_p$  or  $E_d$ ) is absorbed by the sample and that the quantum yield of the acceptor is same in prompt fluorescence and upconverted (delayed) fluorescence. Using either method,  $\Phi_{TTA}$  and  $\Phi_{UC}$  will be dependent on excitation power, increasing with increasing excitation intensity until the strong annihilation limit is achieved. It is also difficult to compare directly measurements performed with continuous wave (cw) excitation and pulsed excitation sources. A pulsed excitation source will have a considerably larger peak power than a cw source with the same average power. For example, a laser with a 10 ns pulse and 10 Hz repetition rate will have a peak power of 100 kW while the average power is only 10 mW.



### 1.3 Scope of Review

With a few exceptions, much of the earlier, pre-2010 work in the sensitized upconversion field has been largely evaluated in room temperature solutions, where the sensitizer and acceptor can diffuse freely [6]. This review will cover more recent developments that have been made over the last 5 years on sensitized upconversion in non-solution environments. These advances are largely in the areas of encapsulating or rigidifying fluid solutions to give them mechanical strength, using inert host materials, and using photoactive materials that incorporate the sensitizer and/or the acceptor. The driving force behind translating upconversion from solution into materials is the incorporation of upconversion into devices and other applications. Some of the most promising applications of upconversion materials at

present include imaging and fluorescence microscopy, photoelectrochemical devices, water disinfection, and solar cells.



## 2 Upconversion in Fluids

### 2.1 Encapsulation

In photochemical upconversion both the TTET and the TTA are diffusional processes, and therefore, are highly sensitive to the viscosity of the surrounding environment. Encapsulating a fluid solution of sensitizer and acceptor in a shell allows the low viscosity and favorable photophysical properties of organic solution to be maintained while garnering the versatility of a solid material along with aqueous and biocompatibility. If the shell has low oxygen permeability, it provides a mechanism to protect the encapsulated solution from oxygen, which quenches both the sensitizer and acceptor triplet states and thereby increases the power threshold for saturation.

Emulsions of hexadecane, containing PdOEP (sensitizer), perylene (acceptor), and polymer precursors, could be thermally polymerized to form polystyrene, poly(methyl methacrylate) (PMMA), or poly(styrene/acrylic acid)-copolymer shells around a liquid hexadecane core containing PdOEP and perylene [10]. The formed core-shell nanocapsules were 150–200 nm in diameter and could be dispersed in water and taken up by HeLa cells. The TTET efficiency between the PdOEP and perylene was reduced compared to solution, as evidenced by the residual phosphorescence. Despite these issues, the upconverted emission intensity was sufficient to visualize HeLa cells with confocal microscopy using cw laser excitation (514 nm,  $\sim 100 \text{ W/cm}^2$ ). While these capsules remained intact in aqueous suspension and when incubated in cells, the fragility of the capsule prevented any dry applications such as thin film formation. Embedding the nanocapsules in poly(vinyl alcohol) PVOH polymer fibers mitigated their fragility and formed a lightweight solid that undergoes upconversion under ambient conditions and is visible to the naked eye [11].

An alternative to thermal polymerization is to use photoinduced polymerization. A solution of PtTPTBP and BPEA in ethoxylated trimethylpropane triacrylate (ETPTA), emulsified in water and irradiated with UV light in a microfluidic channel, formed an ETPTA resin shell around a liquid ETPTA monomer core [12]. The capsule size could be tuned from 210–450  $\mu\text{m}$  by varying the flow rates of the oil and water phases through the microfluidic device and the shell thickness could be varied with irradiation time. Capsules made with this method could be dispersed in water or deposited as a monolayer on a surface. The thinnest shells showed the highest initial upconverted emission intensity, but were susceptible to leakage and quenching by oxygen when exposed to air. Thicker shells were more robust and oxygen stable, but showed decreased upconversion signal and increased phosphorescence from the PtTPTBP trapped in the solid shell.

The Kim group has made more recent advances in UV cured capsules with double [14] and triple [13] layered capsules designed to isolate the chromophores in the liquid core of the capsules. The sensitizer and acceptor are dissolved in mineral oil with polyisobutylene added as an oxygen scavenger (anti-oxidant). The double-layered capsules surround the mineral oil center with an ETPTA shell and the triple layered capsules have a water layer between the oil core and ETPTA shell (Fig. 4). The water layer between the oil and outer shell effectively prevents diffusion of the chromophores from the core into the rigid shell, as evidenced by a significant decrease in sensitizer phosphorescence. These capsules were also highly stable, with the triple layered particles showing <10 % decrease in upconversion intensity after storage in water, under ambient conditions for over 2 months.

A unique approach to encapsulation by Svagan et al. is to use cellulose shells [15]. A hexadecane solution of a mixture of benz- and naphthannulated porphyrin sensitizers and *t*-butylethynyl substituted perylene (TBEP) acceptor was encapsulated in a shell of cellulose nanofibers, and for additional protection from oxygen diffusion, the capsules were imbedded under a thick (8.8  $\mu\text{m}$ ) layer of cellulose nanofibers to form a paper which undergoes upconversion with moderate excitation power densities (<500  $\text{mW}/\text{cm}^2$ , cw excitation). In this upconverting paper, the residual sensitizer phosphorescence was not quenched over 5 h under a 20.5/79.5 oxygen/nitrogen atmosphere. However, the upconverted emission decreased 40 % over 5 h, compared to 80 % over 1.5 h for the unprotected capsules, showing the cellulose nanofibers offer some degree of oxygen protection, but significantly less than rigid polymer shells.

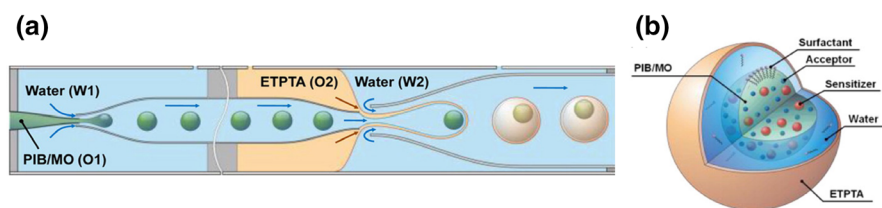


**Fig. 4** Schematic illustration of **a** the microfluidic device used to form triple-layered capsules and **b** the triple layered upconverting capsules. Adapted from Ref. [13]



## 2.2 Organogels

An alternative to encapsulation of fluids inside rigid shells is to provide the fluid solution mechanical stability through gel formation. Gels offer an alternative way to combine the low viscosity of a liquid with the stability and versatility of a solid material. In organogel formation, the gel or crosslinked polymer acts as a host to a liquid solution resulting in a macroscopic solid with microscopic liquid properties. The formation and properties of organogels have been well studied and reviewed [16, 17]. In one example a sorbitol-based gelator (DMDBS) was used with PdTPP and DPA in a tetralin solution [18]. The DMDBS forms a gel consisting of entangled fibril bundles with large volume of interstitial space when heated above 120 °C and cooled to room temperature. The triplet lifetime of PdTPP and the bimolecular quenching constant between the PdTPP and DPA remains unchanged in the gel compared to the tetralin solution, showing the chromophores are still in a solution environment. The TTA quantum yield ( $\Phi_{\text{TTA}}$ ) also remains the same in the gel and liquid solutions, 7 % at one-sun illumination. The gel could be heated and spin coated to form a thin film, but upconversion was quenched on exposure to oxygen.

A gel formed by crosslinking PVOH with hexamethylene diisocyanate (HMDI) (2.5–5 % w/w) in a solution of PdMesoIX and DPA in DMF/DMSO resulted in moldable, free standing gels which undergo photon upconversion even when prepared and measured under ambient conditions [19]. Gels prepared and measured under air free conditions had an upconversion quantum yield ( $\Phi_{\text{UC}}$ ) of approximately 14 % ( $\lambda_{\text{ex}} = 543 \text{ nm}$ , 180 mW/cm<sup>2</sup>, cw excitation). This quantum yield decreased significantly when the gels were prepared and measured under ambient conditions, but the upconverted emission was still visible to the eye. When the gel was frozen (77 K) the upconverted emission disappeared and only PdMesoIX phosphorescence was observed, confirming that upconversion is the result of molecular diffusion in the room temperature gel.

To gain additional oxygen resistance *N,N'* bis(octadecyl)-*L*-*boc*-glutamicdiamide (LBG) was used a gelator [20]. LBG creates a gel by forming a network of interconnecting, vesicle-like nanofibers with the upconverting solution inside the fiber (Fig. 5). Solutions of PtOEP and DPA in DMF were gelled with LBG by heating to uniformly dissolve all components and cooling to room temperature. This method yielded moldable, freestanding gels that showed no significant decrease in UC intensity even after 25 days of air exposure. Upconversion also occurs at very low power density, with an  $I_{\text{th}}$  of 1.48 mW/cm<sup>2</sup> in the aerated gel. The upconversion was also thermally reversible, heating to 90 °C above the gel temperature, decreases the upconversion efficiency and cooling to 25 °C recovers the upconversion intensity. This is reproducible over many heating and cooling cycles, but prolonged (<2 h) heating in air leads to a permanent decrease in upconversion efficiency presumably due to increased oxygen diffusion into the hot solution. This gelation method was also shown to be applicable to a range of different sensitizer and acceptor combinations, spanning from yellow to UV emission (Fig. 6). These gels show impressive oxygen stability and a low power threshold, but, as they are solution based, long-term use over months or years without solvent loss might be a potential issue.

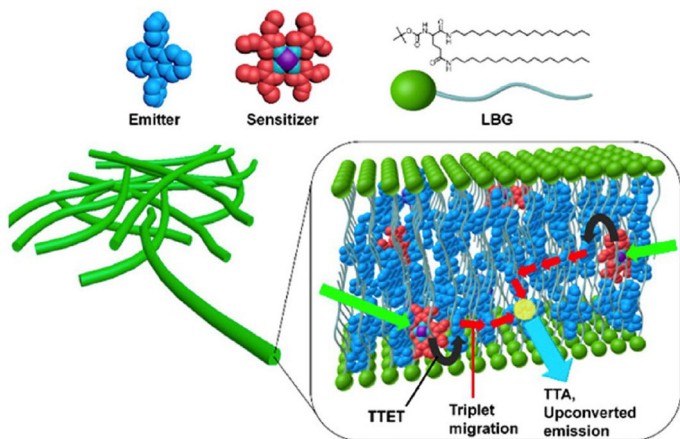


**Fig. 5** Illustration of upconverting organogel formed from *N,N'* bis(octadecyl)-*L*-*boc*-glutamicdiamide (LBG). Reprinted with permission from Duan P, Yanai N, Nagatomi H, Kimizuka N (2015) *J. Am. Chem. Soc.* 137:1887–1894. Copyright 2015 American Chemical Society

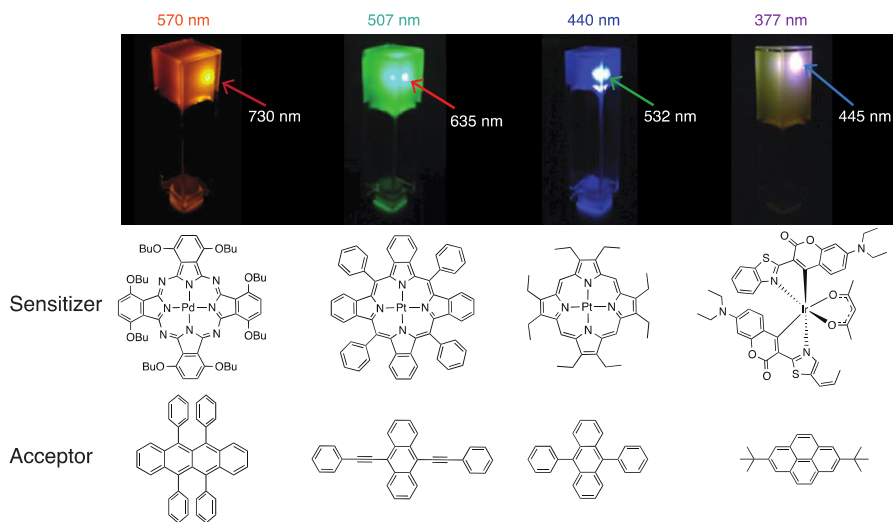


**Fig. 6** Digital photographs of sensitizer and acceptor combinations in LBG organogels. Adapted from Ref. [20]

### 3 Inert Substrates

#### 3.1 Soft Materials

A flexible, rubbery polymer is the material environment that is closest to a fluid solution. The sensitizer and acceptors are guests inside the polymer matrix and

(slow) diffusion can occur through the polymer. The first and most successful examples of upconversion in solid materials used low  $T_g$  polymers such as ethylene oxide and epichlorohydrin copolymers and thermoplastic polyurethanes [21, 22]. More recent examples embed the sensitizer and acceptor in a soft polyurethane polymer (ClearFlex 50) [23] and poly butylacrylate elastomer [24]. Previous polymer work has relied on soaking or dissolving the preformed polymer in a solution of sensitizer and acceptor followed by removal of solvent. The advantage of these newer polymer systems is that the sensitizer and acceptor can be mixed with the polymer precursors prior to polymerization. This allows for precise control over the concentration of both components and ensures they are evenly distributed throughout the final polymer. Additionally, any desirable shape or size can be constructed in these instances. Both of the final polymers films show impressive upconversion quantum yields ( $\Phi_{UC} = 22\%$  for ClearFlex 50 and  $17\%$  for poly butylacrylate) at moderate cw excitation intensities ( $200\text{ mW/cm}^2$  for ClearFlex 50 and  $100\text{ mW/cm}^2$  for poly butylacrylate) under ambient conditions.

### 3.2 Rigid Materials

Moving from a flexible polymer into a rigid material offers some challenges. In a rigid environment, molecular diffusion isn't a viable mechanism for TTET or TTA. Instead, one needs to rely on energy/exciton diffusion, which requires higher chromophore concentrations to overcome short exciton diffusion lengths. Initial work demonstrated that upconversion was indeed possible in rigid films, but the efficiency was much less than in fluid solution [25, 26]. Lee and co-workers dissolved PdOEP (0.005–0.5 wt%) and DPA (25 wt%) in molten PMMA and pressed it into a 100–180  $\mu\text{m}$  thick film, which was rapidly cooled to form an optically transparent glass with a uniform distribution of chromophores [27]. Decreased upconversion efficiency was observed in films with higher loadings of PdOEP, as seen in Fig. 7. This is presumably due to the aggregation of the PdOEP in the polymer and subsequent formation of low-energy triplet trap states. Films were stable when stored in the dark under ambient conditions for up to 3 months. In the 0.05 % w/w PdOEP film, nearly linear power dependence (slope = 1.2) was observed at cw excitation power densities as low as  $34\text{ mW/cm}^2$ . Linear power dependence in upconversion requires significant control of experimental parameters, particularly in fluid solution, but conditions exist in the solid state that make it more likely to be observed. In the PMMA film, molecular oxygen was excluded due to the low oxygen permeability of PMMA and in a rigid solid the non-radiative decay of the sensitizer and acceptor was significantly restricted. These factors, combined with high concentration of DPA (500x [PdOEP]), decrease  $k_T$  and increase  $k_{TT}[^3A^*]$ , which lowered the power threshold required to achieve the strong annihilation limit.

A theoretical study has simulated triplet–triplet annihilation in two different arrangements of sensitizers and acceptors in an inert host [28]. In the first arrangement, the sensitizer and acceptor are randomly distributed through the host matrix and in the second arrangement the sensitizers are clustered in islands surrounded by acceptors. The model simulates the creation of the sensitizer excited state, triplet diffusion via a hopping mechanism, TTET between sensitizer and

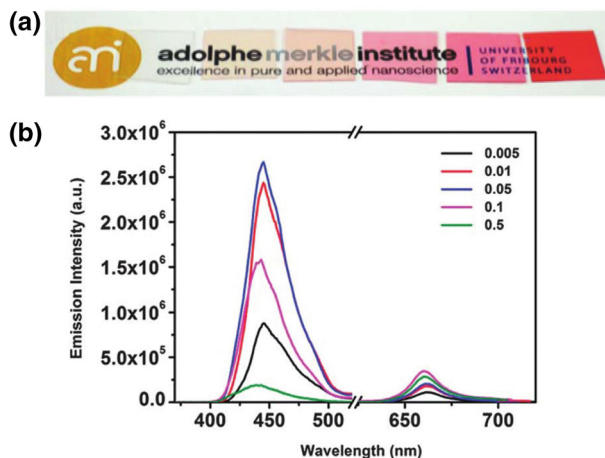


**Fig. 7** **a** Digital photograph of, from left to right, neat PMMA and films containing 25 wt% DPA and 0.005, 0.01, 0.05, 0.1, and 0.5 wt% PdOEP. **b** Emission spectra of the PdOEP/DPA containing films with 543 nm excitation (340 mW/cm<sup>2</sup>), wt% of PdOEP is given in the legend. Adapted from Ref. [27]

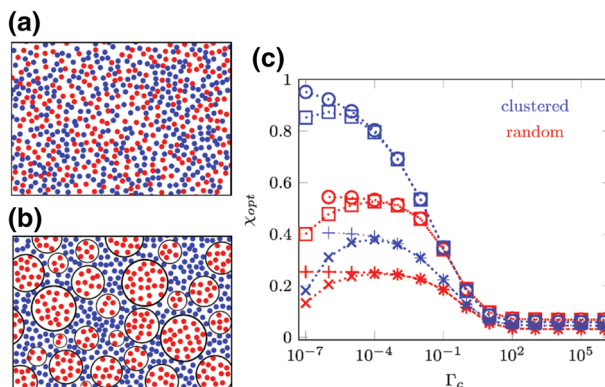


**Fig. 8** Illustration of the **a** random and **b** clustered arrangements of sensitizers (red) and acceptors (blue). **c** Optimal upconversion efficiencies ( $\chi_{opt}$ ) vs. excited state creation rate ( $\Gamma_c$ ) for the random (red) and clustered (blue) arrangements. Symbols represent different sets of simulation parameters. Adapted from Ref. [28]

acceptor, and TTA of two triplet acceptors as well as the non-productive TTA of two sensitizers, TTA of one sensitizer and one acceptor, and the decay of both triplet states. In both arrangements, and under all simulation conditions, the upconversion quantum efficiency ( $\chi_{opt}$ ) decreased as the rate of excited state creation ( $\Gamma_c$ ) increased. In the high creation rate region, TTA between sensitizer triplets that result in the non-productive loss of sensitizer triplets, becomes the dominant decay pathway. In the low creation rate region, however, the clustered arrangement outperforms the random arrangement under all the tested conditions (Fig. 8). This is because, in the random distribution, many acceptor triplets were

formed in isolation and decayed before they encountered another acceptor triplet, whereas in the clustered distribution acceptor triplets were localized around the sensitizer islands. This result suggests that, especially under low light conditions, an ordered arrangement of sensitizer and acceptor is superior to a random distribution. A caveat of this result is that the simulations did not take into account the aggregation of sensitizers and formation of triplet trap states that are observed in experimental devices.

### 3.3 Nanoparticles

One solution to short exciton diffusion lengths in solid materials is to use nanoparticles rather than rigid films. In an example from Monguzzi and co-workers, PtOEP and DPA were imbedded in pre-formed polystyrene nanoparticles 16 nm in diameter by soaking in a solution containing PtOEP and DPA then rinsing and removing excess organic solvent [29]. The dye loading was, on average, one PtOEP molecule and 50 DPA molecules per nanoparticle as measured by UV–visible absorption. The polystyrene and stabilizing surfactant are both effective barriers against oxygen, upconversion could be observed in aqueous suspensions and thin films exposed to air. The residual photoluminescence decay of the PtOEP was biexponential, indicating the PtOEP was in two local environments, one where TTET to the DPA was possible (8.9  $\mu\text{s}$  component) and one where TTET to DPA wasn't possible (71.2  $\mu\text{s}$  component). These results suggested that  $\sim 75\%$  of the excited PtOEP chromophores successfully undergo TTET to the DPA. Kinetic analysis of the unconverted DPA emission showed a rise time of 16.4  $\mu\text{s}$ , approximately twice the rate of TTET from PtOEP to DPA. This is a good indication that the  $^3\text{DPA}^*$  is formed by energy transfer from the  $^3\text{PtOEP}^*$ . Power dependence measurements using a pulsed excitation source also found that the strong annihilation limit can be reached at low excitation intensities (5.6  $\text{mW}/\text{cm}^2$ ). Most interestingly, this study found no differences in performance between aqueous suspensions and thin films of the nanoparticles, showing that each particle acts independently and increasing the concentration of particles has no negative effect on performance. This offers a mechanism to increase chromophore concentration (and light absorption) without aggregation and trap state formation.

Taking a different approach to photochemical upconversion with nanoparticles, the Morandeira group studied upconversion on the surface of nanocrystalline  $\text{ZrO}_2$  films with the hopes of transferring the technology to  $\text{TiO}_2$  and generating photocurrent rather than emission from TTA. Physisorbing PtOEP and DPA onto sintered films of  $\text{ZrO}_2$  nanoparticles lead to a very weak ( $\Phi_{\text{UC}} = 6 \times 10^{-4} \%$ ) upconverted emission signal under non-coherent, low intensity (8  $\text{mW}/\text{cm}^2$ ) illumination due to aggregation of PtOEP and poor orientation of the DPA on the nanoparticle surface [30]. This poor efficiency was improved by covalently linking the DPA to the  $\text{ZrO}_2$  surface through a carboxylate anchor, forcing them to align perpendicular to the  $\text{ZrO}_2$  surface [31, 32]. The PtOEP sensitizer was dissolved in butyronitrile, and the film and sensitizer solution were sealed under an inert atmosphere. This device architecture showed improved upconversion efficiency ( $\Phi_{\text{UC}} = 0.04 \%$ ) under non-coherent, low intensity (8  $\text{mW}/\text{cm}^2$ )

illumination, and power dependence measurements showed that the device deviated from the weak annihilation limit at intensities  $<10 \text{ mW/cm}^2$ . However, the relatively thick pathlength of the device ( $50 \mu\text{m}$ ) meant that only a small fraction ( $\sim 3 \%$ ) of the excited PdOEP was close enough to the surface to undergo TTET with the surface bound DPA. Anchoring the sensitizer to the nanoparticle surface, rather than relying on diffusion, could potentially lead to further performance improvements.

## 4 Photoactive Substrates

### 4.1 Thin Films

Rather than embedding sensitizer and acceptor materials in an inert material, using neat films of sensitizer and acceptor materials represents one method to improve triplet exciton diffusion through the material. Karpicz and co-workers doped thin films of DPA with PtOEP and studied them with transient absorption spectroscopy to probe triplet exciton diffusion [33]. The authors found that ISC in PtOEP was faster than the 100 fs experimental resolution, much faster than what was observed in PdTPPTBP [34]. Also, crystallization of the DPA and concomitant formation of PtOEP domains lead to slow energy transfer between the PtOEP and DPA. Interestingly, unlike other studies [27, 34, 35], there was no evidence of non-productive TTA within the PtOEP domains. Rather than the traditional inorganic sensitizer, Baldo and co-workers used an organic semiconductor (4CzTPN-Ph) to sensitize a thin film of DPA [36]. The advantage of the 4CzTPN-Ph sensitizer is that it has a comparatively small singlet–triplet gap ( $\Delta E_{ST} < 800 \text{ cm}^{-1}$ ), meaning ISC occurs without a heavy atom and less excitation energy is lost through ISC. A device formed of a 50 nm film of DPA, topped with a 20 nm film of 4CzTPN-Ph did produce upconverted emission when excited at 532 nm. The efficiency was limited by both the poor absorption of the 4Cz-TPN-Ph, which only absorbed 6.8 % of the excitation light, and poor energy transfer to the DPA ( $\Phi_{\text{TTET}} = 9.1 \%$ ). Despite the low efficiency, the magnetic field dependence of the upconverted emission was able to confirm that the emission was likely a result of TTA.

### 4.2 Sensitizer and Acceptor Materials

A strategy in upconverting materials is to incorporate photoactive components, either the sensitizer or acceptor into the host matrix rather than using an inert material. Jankus and co-workers used the commercially available fluorescent poly(paraphenylene vinylene) polymer, super yellow, doped with PdTPPTBP, looking towards applications in organic photovoltaic devices [34]. Toluene solutions of the super yellow and PdTPPTBP were drop cast to form thin films that were 4 wt% PdTPPTBP. Ultrafast transient absorption studies of the films reveals intersystem crossing in the PdTPPTBP, with a time constant of 5.7 ps, as well as TTET to the polymer, with a time constant of 930 ps. Nanosecond studies

revealed, however, that a majority of the excited PdTPTBP was decaying through self-TTA rather than TTET to the polymer. This indicates that the sensitizer was indeed aggregated in the polymer. This was supported by the broadened absorption spectrum of the PdTPTBP in super yellow compared to solution. Kinetic analysis of the delayed fluorescence showed that the TTET yield ( $\Phi_{\text{TTET}}$ ) was at best 24 % and the  $\Phi_{\text{UC}}$  was 6 %.

Building on their previous work on PMMA films [27] Weder, Simon and co-workers have developed a method to incorporate DPA into the PMMA polymer [37]. Methacrylate-substituted DPA (DPAMA) was co-polymerized with methyl methacrylate, yielding polymers with a DPA content that ranged from 8 to 54 wt%. Glassy films with 0.05 wt% PdOEP were formed with thickness ranging from 50–250  $\mu\text{m}$ . The optimal DPA content, as measured by upconverted emission intensity, was found to be 34 wt% due to self-quenching to the DPA fluorescence at higher concentrations. The optimal film (34 wt% DPA and 0.05 wt% PdOEP) also proved to be both air and photo-stable, showing stable upconverted emission over 3.5 h of continuous irradiation, after 4 months of aging. The advantage of incorporating the DPA into the polymer backbone is that a higher concentration of DPA can be used without phase separation or crystallization of the DPA in the polymer film, allowing for quantitative TTET from the PdOEP to the DPA.

Another way to incorporate chromophores into a solid material without aggregation is to use metal–organic frameworks (MOFs). A zinc-based MOF, using 4,4'-(anthracene-9,10-diyl)dibenzoate (ADB) as the bridging ligand was synthesized and sensitized with PtOEP [38]. In the MOF structure, the anthracene cores of the ADB are stacked co-facially and separated by 9 Å, as shown in Fig. 9. This arrangement allows for efficient triplet exciton diffusion along the MOF lattice without aggregation. When the ADB containing MOFs are dispersed in a deaerated solution containing PtOEP as a sensitizer upconverted emission at 440 nm can be observed with 532 nm excitation. The MOF could also be sensitized by exchanging carboxylates on the MOF surface with PdMesoIX. The resulting MOF was imbedded in PMMA, resulting in

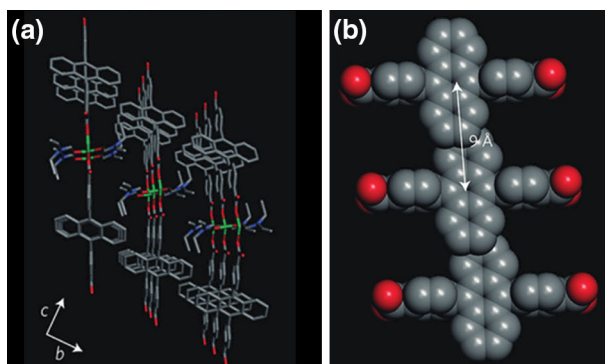


**Fig. 9** a Crystal structure of the synthesized Zn-ADB MOF b Arrangement of ADB ligands in the MOF structure. Adapted from Ref. [38]

stable photon upconversion with a threshold power density of  $<1 \text{ mW/cm}^2$ . These sensitized and encapsulated MOF structures offer an exciting combination of excitation powers accessible by solar irradiance and reasonable quantum efficiencies ( $\Phi_{\text{UC}} = 1.9 \%$  with  $5 \text{ mW/cm}^2$  excitation).

Rather than being detrimental to upconversion, aggregation can also be used to enhance the upconversion process [39]. Cyano-substituted 1,4-distyrylbenzene (CN-DSB) was used as a triplet acceptor for PtOEP. In solution TTET from the PtOEP to the CN-DSB is quantitative; however, no upconverted emission is observed and no long-lived CN-DSB triplet excited state can be detected by nanosecond transient absorption spectroscopy. Crystalline thin films of CN-DSB doped with PtOEP did, however, produce upconversion under an inert atmosphere (Fig. 10) at relatively low excitation power densities ( $I_{\text{th}} = 14.5 \text{ mW/cm}^2$ ). In solution, the triplet state of CN-DSB is deactivated very rapidly through a conformational twisting around a C=C bond. In the solid state, the rigid environment prevents twisting and the resulting long-lived CN-DSB triplet states can undergo annihilation. These results show that acceptors that undergo aggregation-induced emission (AIE) are also viable candidates for photon upconversion and offer a way to work at high acceptor concentrations without enhancing non-productive acceptor decay pathways.

The natural extension of incorporating the acceptor into a material is to incorporate both species into the same material. In one example, PdMesoIX and DPA-(CH<sub>2</sub>OH)<sub>2</sub> were used as cross-linkers in poly(mannitol-sebacate) as shown in Fig. 11 [40]. This resulted in a rubbery polymer with 0.05 wt% PdMesoIX and 34 wt% DPA which exhibited blue fluorescence when excited at 543 nm ( $32\text{--}320 \text{ mW/cm}^2$ ). However, in the crosslinked polymer there was also a significant amount of unquenched phosphorescence from PdMesoIX indicating inefficient TTET between the sensitizer and acceptor. The polymer used is a soft elastomer, meaning molecular diffusion is possible through the polymer matrix, linking the sensitizer and acceptor to the polymer eliminates molecular diffusion. The TTET and TTA processes must therefore rely on triplet exciton diffusion through the polymer.

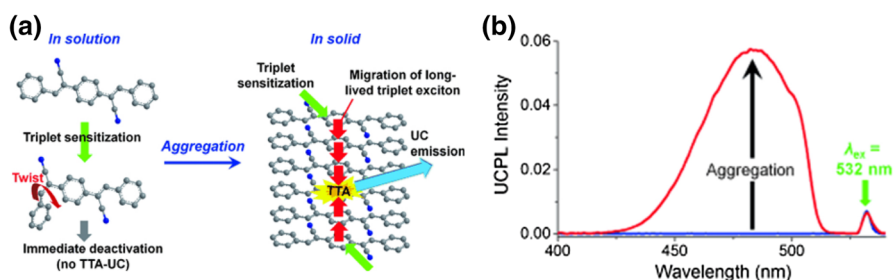


**Fig. 10** **a** Schematic illustration of aggregation induced upconversion with CN-DSB. In solution the triplet state is deactivated through *cis-trans* isomerization before it can undergo TTA. In the solid state isomerization is restricted and the triplet states undergo TTA. **b** Upconverted emission spectra of PtOEP and CN-DSB in degassed THF solution (blue) and in a solid film (red). Adapted from Ref. [39]



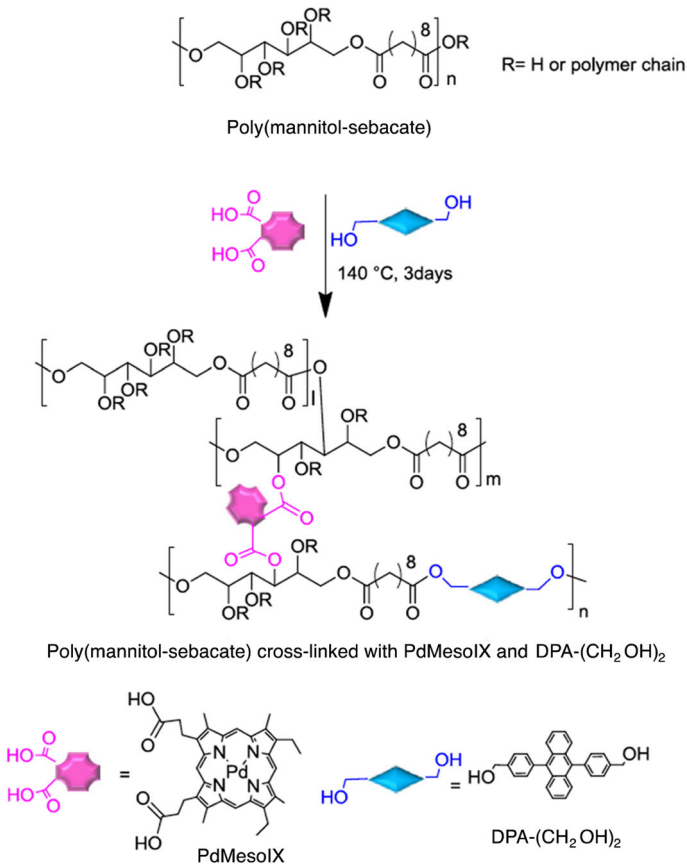


**Fig. 11** Incorporation of PdMesolX and DPA-(CH<sub>2</sub>OH)<sub>2</sub> into a poly(mannitol-sebacate) copolymer. Adapted from Ref. [40]

## 5 Applications and Device Integration

### 5.1 Photovoltaic Devices

Photon upconversion has long been recognized as a potential mechanism for solar cells to use sub-bandgap photons, potentially exceeding the imposed Shockley-Queisser limit [41–47]. Incorporating an upconverting layer into a single junction photovoltaic device increases the maximum theoretical efficiency from ~30 to ~45 % under 1 sun illumination and allows for wider bandgap materials to be used, as shown in Fig. 12 [41, 43]. Schmidt, Lips, and co-workers have successfully incorporated photon upconversion layers into amorphous silicon [48–50], organic [48], and dye sensitized [51] photovoltaic devices. In these devices, air-free solutions of a red-absorbing sensitizer, PQ<sub>4</sub>Pd or PQ<sub>4</sub>PdNA, and rubrene acceptor were sealed in a 1 cm pathlength cuvette and mounted on the backside of the device

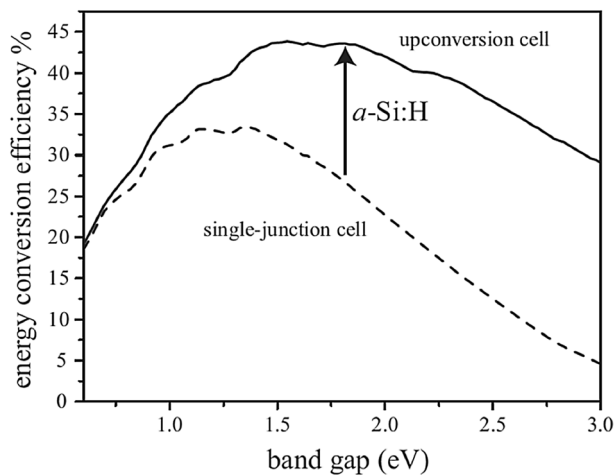


**Fig. 12** The energy conversion limits for a single junction photovoltaic device (*dashed line*) and an upconverting single junction photovoltaic device (*solid line*) under 1 sun illumination as a function of bandgap. Reprinted with permission from [41]. Copyright 2013 Society of Photo Optical Instrumentation Engineers

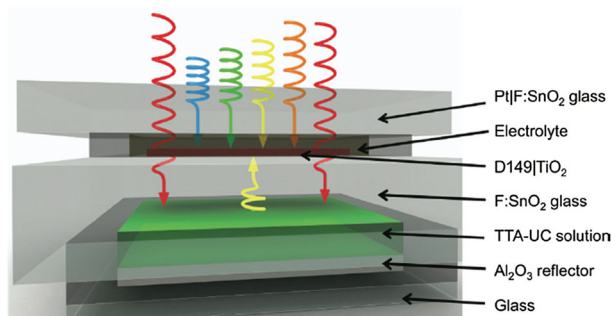


**Fig. 13** Diagram illustrating the incorporation of an upconversion solution into a dye-sensitized solar cell. Reprinted with permission from Nattestad A, Cheng YY, MacQueen RW, Schulze TF, Thompson FW, Mozer AJ, Fückel B, Khoury T, Crossley MJ, Lips K, Wallace GG, Schmidt TW (2013) *J. Phys. Chem. Lett.* 4:2073–2078. Copyright 2013 American Chemical Society

as shown in Fig. 13. In this arrangement, long wavelength light not absorbed by the photovoltaic device passes through to be absorbed by the upconversion solution. The upconverted emission is reradiated and can be absorbed by the photovoltaic material. These devices all showed small but significant increases in photocurrent, ranging from  $2.25 \times 10^{-3}$  to  $0.275 \text{ mA/cm}^2$  and plots of incident photon-to-current efficiency vs. wavelength showed the increased photocurrent is due to light absorbed by the upconversion solution. While using a cuvette of upconverting solution is not practical device integration, these studies show that even with non-ideal integration upconversion can yield real and measurable improvements in photovoltaic devices of all types.

## 5.2 Photocatalysis

The idea of photocatalysis is similar to photovoltaic devices, but in this case the energy of the absorbed light performs a chemical reaction rather than generating electricity. Direct excitation of wide bandgap semiconductors such as  $\text{TiO}_2$  and  $\text{WO}_3$  produces an oxidizing valence band hole and reducing conduction band electron, capable of many useful chemical transformations such as water oxidation and water detoxification. Unfortunately, UV light is needed to excite these semiconductors, meaning they use very little of the available sun's solar spectrum. Photon upconversion can be an asset in these applications by converting visible light into UV light that can be absorbed by the semiconductor.

As a proof-of-principle, Khnayzer et al. used an air-free solution of PdOEP and DPA to sensitize a  $\text{WO}_3$  photoanode as shown in Fig. 14 [52]. Under non-coherent visible illumination ( $\lambda > 500 \text{ nm}$   $32 \text{ mW/cm}^2$ ) the upconversion solution produces Anti-Stokes fluorescence between 400 and 450 nm, which is stochastically collected by the  $\text{WO}_3$  electrode. With a small positive bias (0.9 V vs. Ag/AgCl) the  $\text{WO}_3$  electrode was capable of oxidizing water and producing a photocurrent. Control

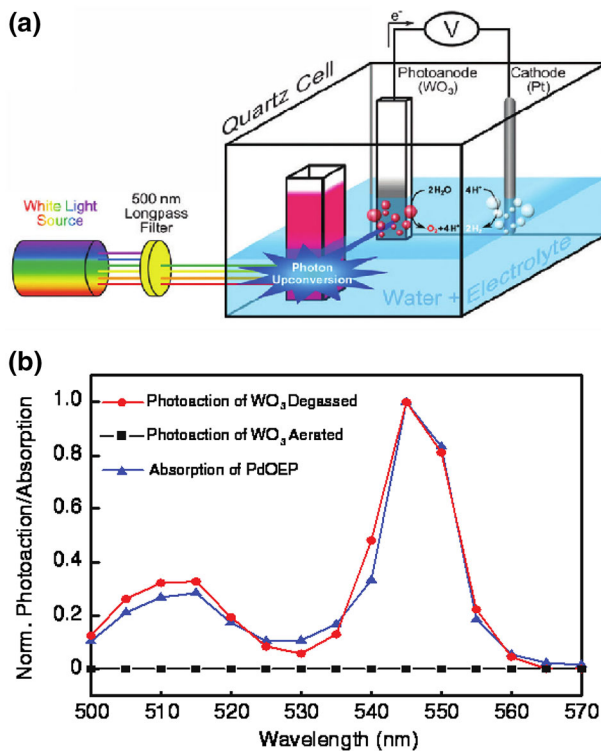


**Fig. 14** **a** Schematic illustration of an upconversion-powered photoelectrochemical cell. **b** Normalized photoaction spectra of the photoelectrochemical cell with a degassed (red circles) and aerated (black squares) upconversion solution compared to the absorption spectrum of the PdOEP sensitizer (blue triangles). Adapted from Ref. [52]

experiments using a non-upconverting, air saturated solution of PdOEP and DPA did not produce photocurrent. A photoaction spectrum of the device in the visible region also matches the absorption spectrum of the PdOEP sensitizer. Together these experiments show that the upconversion solution is able to convert visible light into UV light, which is absorbed by the photoanode to generate photocurrent.

The Kim group expanded on this result by using upconverting microcapsules to sensitize platinum-loaded  $\text{WO}_3$  nanoparticles [53]. Microcapsules containing PdOEP and DPA were suspended with the Pt/ $\text{WO}_3$  nanoparticles in an aqueous solution and irradiated with a 532 nm laser. The photochemical formation of hydroxyl radicals was detected by the formation of the emissive 7-hydroxycoumarin from coumarin. Control experiments without the upconverting microcapsules resulted in no hydroxyl radical formation. Similarly, Vaiano and co-workers coated upconverting silica nanoparticles containing PdOEP and DPA with n-doped  $\text{TiO}_2$  nanoparticles. Under green or white LED excitation the particles were capable of decolorizing many common dyes such as methylene blue, crystal violet, and Rhodamine B. This type of semiconductor based photochemistry is important in both solar fuels photoelectrochemistry, where the semiconductor electrode will catalyze fuel-forming reactions and in solar water detoxification, where the semiconductor particles will generate reactive oxygen species such as hydroxyl radicals which then go on to degrade organic and inorganic pollutants and deactivate pathogens in drinking water.

### 5.3 Fluorescence Imaging

Fluorescence imaging, particularly in biological samples, is another application where photon upconversion has great potential to be useful. Using an upconverting dye rather than a traditional fluorescent dye allows for an anti-Stokes detection window, which minimizes or eliminates background sample fluorescence. Upconversion also allows the excitation to shift into the biological window ( $\sim 650 - 1300$  nm) where the light penetration depth into tissue is the largest while keeping the emission in the more easily detected visible region. Nanoscale upconversion systems, either encapsulated solutions or solid nanoparticles have proven to be readily used in imaging applications.

As mentioned previously, Wohnhaas et al. have used polystyrene-acrylic acid copolymer nanocapsules containing PdOEP and perylene in a hexadecane solution to visualize HeLa cells. The capsules were small enough that they were taken into the cells after incubation [10]. Li and co-workers developed biocompatible silica nanoparticles containing PdOEP and DPA as the sensitizer and acceptor [54]. Dispersed in water these particles had an upconversion quantum yield of 4.5 % ( $\lambda_{\text{ex}} = 532$  nm, 260 mW/cm<sup>2</sup>) and showed no photobleaching after 30 min of continuous irradiation. These upconverting nanoparticles were used to stain live HeLa cells and perform in vivo lymphatic imaging in a live mouse. To avoid problematic aggregation with more red absorbers and emitters the authors shifted from solid nanoparticles to nanocapsules with liquid cores [55]. A water stable and bio-compatible shell of dextran and bovine serum albumin contained sensitizers and acceptors in soybean oil. The red absorbing PtTPTBP could be combined with green

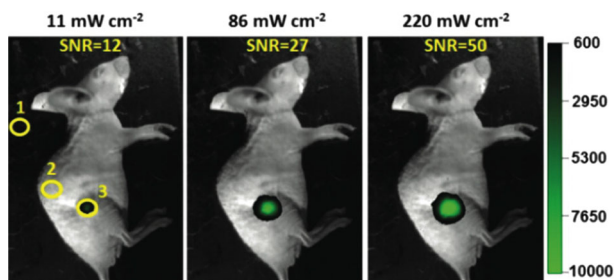


**Fig. 15** In vivo fluorescence imaging of live mouse after subcutaneous injection of BD-G containing nanocapsules under different excitation power densities ( $\lambda_{\text{ex}} = 635$  nm). The signal-to-noise ratio (SNR) is given for each power density. Reprinted with permission from Liu Q, Yin B, Yang T, Yang Y, Shen Z, Yao P, Li F (2013) *J. Am. Chem. Soc.* 135:5029–5037. Copyright 2013 American Chemical Society

(BD-G) or yellow (BD-Y) emitting boron dipyrromethene dyes to form red-to-green and red-to-yellow upconverting nanocapsules. Aqueous suspensions of these nanocapsules under ambient conditions showed quantum yields of 1.7 % (BD-G) and 4.8 % (BD-Y) under moderate excitation intensities ( $\lambda_{\text{ex}} = 635$  nm, 106 mW/cm<sup>2</sup>). As with the previously reported Si nanoparticles, the nanocapsules were capable of in vivo fluorescence imaging in live mice with excitation intensities as low as 12 mW/cm<sup>2</sup> (Fig. 15).

#### 5.4 Other Emerging Applications

While the above applications are the ones most commonly studied with photochemical upconversion they are not the only viable candidates. Similar to biological imaging, photodynamic therapy is a technique which can benefit from the incorporation of photon upconversion. In photodynamic therapy a drug or prodrug is activated by the absorption of light. Upon absorption of light the drug can produce reactive singlet oxygen species, form an activated drug that can damage cells/DNA or some combination of both. The difficulty of photodynamic therapy is that the visible wavelengths of light often needed for this chemistry have very limited penetration through tissue. Incorporating upconversion into photodynamic therapy allows for red or NIR excitation. Bonnet and co-workers have created upconverting PEGylated liposomes containing PdTPTBP and perylene as the sensitizer and acceptor [56]. These upconverting liposomes were mixed with ruthenium-functionalized liposomes, which contained a photoactivatable ruthenium complex  $[\text{Ru}(\text{tpy})(\text{bpy})(\text{SRR}') ]^{2+}$  (tpy = 2,2':6',2''-terpyridine, bpy = 2,2'-bipyridine, SRR' = thioether-cholesterol ligand). Irradiation with blue light cleaves the Ru–S bond and frees  $[\text{Ru}(\text{tpy})(\text{bpy})(\text{H}_2\text{O}) ]^{2+}$  from the liposome. Irradiation of the mixture of liposomes with red light ( $\lambda_{\text{ex}} = 630$  nm) lead to the formation of  $[\text{Ru}(\text{tpy})(\text{bpy})(\text{H}_2\text{O}) ]^{2+}$  in solution (Fig. 16). This photo-induced release strategy is well suited to photodynamic therapy agents, or could be used to use to encapsulate and release traditional drugs in selected areas or the body.

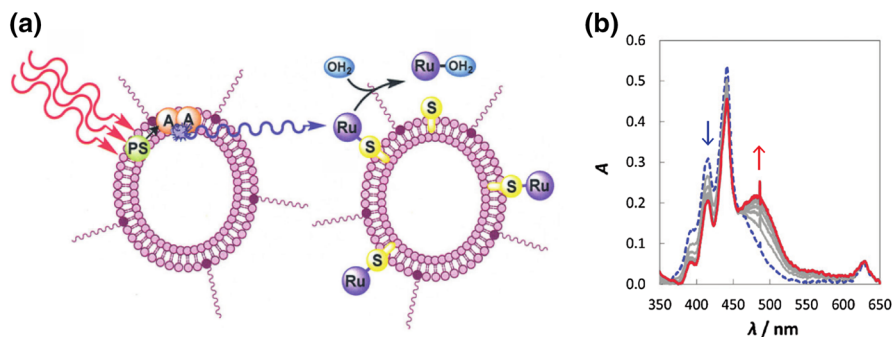


**Fig. 16** **a** Schematic illustration of photon upconversion in the liposome bilayer followed by photo-release of  $[\text{Ru}(\text{tpy})(\text{bpy})(\text{H}_2\text{O})]^{2+}$ . **b** Absorption spectra of liposome mixture during photolysis showing the formation of  $[\text{Ru}(\text{tpy})(\text{bpy})(\text{H}_2\text{O})]^{2+}$  at 490 nm. Blue dashed line is at  $t = 0$  and red solid line is at  $t = 240$  min. Adapted from Ref. [56]

It is well known that the sensitized photon upconversion process is highly sensitive to oxygen, making it an ideal oxygen sensor. Upconverting solutions containing PtTPTBP or PdTPTBP as the sensitizer and Solvent Green 5 (SG-5) were adsorbed into porous glass beads and imbedded into an oxygen permeable polymer (silicon or Teflon AF) [57]. Because the upconversion device has two modes of emission, upconverted fluorescence and residual phosphorescence from the sensitizer it is capable of accurately detecting oxygen over a much wider dynamic range ( $\text{pO}_2$  trace—40 kPa) than traditional oxygen sensors. At low oxygen concentrations ( $<0.2$  kPa  $\text{O}_2$ ) the upconverted fluorescence shows significant quenching, and nearly quantitatively quenched by 1 kPa  $\text{O}_2$ . The residual phosphorescence signal is much less sensitive; the emission signal is detectable at concentrations as high as 40 kPa  $\text{O}_2$ . Unfortunately, the SG-5 also proved susceptible to photodegradation by singlet oxygen, and devices degraded under constant illumination in the presence of oxygen. Moving from a perylene-type acceptor to one more resistant to degradation in the presence of oxygen is a relatively simple way to improve the long-term stability of these materials.

## 6 Future Directions

To further improve upon photochemical upconversion in materials, and its incorporation into devices and other applications there are several factors to consider. For all types of usages, with the exception of oxygen sensing, exclusion of oxygen is critical for both maximizing upconversion efficiency and long-term stability. This has been achieved either through oxygen impermeable materials, or by the addition of oxygen scavengers. In biological applications such as imaging and photodynamic therapy, water and biological compatibility as well as low toxicity represent important mandated properties. Long-term stability over months or years is not required for these applications, especially when used in living

subjects. Ideally, after the imaging or drug delivery process has been completed, the upconverting materials would ideally break down and/or be excreted from the body. Further development of materials with small particle sizes that can cross membranes into cells and materials with target-specific coatings for localized drug delivery or imaging represent desirable goals for future research endeavors. In biological applications, low power thresholds are not critical because ambient light (or solar photons) isn't the desired excitation source, but using excitation wavelengths suitable for biological tissue windows is important. For integration into solar cell and photocatalysis devices, long-term stability over years of operation appears crucial. This potentially limits the use of fluidic-based materials such as organogels. In order for these devices to operate using the solar spectrum as the excitation source, a low power threshold is required to get the maximum upconversion efficiency out of low excitation power densities. In photovoltaic devices the sensitizer absorption should be in the red and NIR, below the bandgap of the photovoltaic material, and the acceptor emission should be efficiently absorbed by the photovoltaic material (i.e., within the bandgap). In photocatalytic upconversion applications combinations of sensitizers and acceptors that convert the visible light of the solar spectrum into UV light that can sensitize wide-bandgap semiconductors are also needed.

One major difficulty of incorporating upconversion into materials is need for molecular diffusion. As of yet, none of the reported solid upconversion materials come close to matching the upconversion quantum yields that have been reported in solution or soft polymers, where molecular diffusion is readily enabled. These solid materials must rely on triplet exciton diffusion for both TTET and TTA, meaning concentrations of sensitizer and acceptor used must be significantly higher than in solution. Theoretical studies suggest that the best way to overcome this is to have ordered domains of sensitizer and acceptor so that TTET and TTA can occur at or near the interface between sensitizer and acceptor domains. In experimental devices, however, sensitizer aggregation and trap state formation, as well as acceptor self-quenching ultimately limit material performance.

Considering all of the work completed on upconverting materials there has been a very limited selection of sensitizer and acceptor chromophores that have been evaluated. With few exceptions the sensitizers have remained in the Pt(II) and Pd(II) porphyrin family and the acceptors are mostly anthracene derivatives although other polycyclic aromatic hydrocarbons have been investigated. Diversifying the selection of chromophores used in photochemical upconversion materials should enable marked expansion of excitation and emission wavelengths while minimizing aggregation in sensitizers and/or acceptors in addition to improving oxygen stability of the requisite compositions. The recent observation of triplet-triplet energy transfer from semiconductor nanocrystals to molecular acceptors [58] implies new classes of triplet sensitizers are immediately available for incorporation in upconversion schemes.

**Acknowledgments** This material is based upon work supported by the U.S. Department of Energy, Office of Science, Office of Basic Energy Sciences, under Award Number DE-SC0011979. Some of the work on solid-state upconversion performed in this laboratory was supported by the Air Force Office of Scientific Research (FA9550-13-1-0106).

## References

1. Parker CA, Hatchard CG (1962) *Proc Chem Soc London*, pp 386–387
2. Parker CA (1963) *Proc R Soc A* 276:125–135
3. Parker CA, Hatchard CG, Joyce TA (1964) *J Mol Spectrosc* 14:311–319
4. Kozlov DV, Castellano FN (2004) *Chem Commun*, pp 2860–2861
5. Islangulov RR, Kozlov DV, Castellano FN (2005) *Chem Commun*, pp 3776–3778
6. Singh-Rachford TN, Castellano FN (2010) *Coord Chem Rev* 254:2560–2573
7. Haefele A, Blumhoff J, Khnayzer RS, Castellano FN (2012) *J Phys Chem Lett* 3:299–303
8. Montalti M, Credi A, Prodi L, Gandolfi MT (2006) *Handbook of photochemistry*, 3rd edn. CRC Press, Boca Raton
9. Cheng YY, Khoury T, Clady RG, Tayebjee MJ, Ekins-Daukes NJ, Crossley MJ, Schmidt TW (2010) *Phys Chem Chem Phys* 12:66–71
10. Wohnhaas C, Turshatov A, Mailander V, Lorenz S, Balushev S, Miteva T, Landfester K (2011) *Macromol Biosci* 11:772–778
11. Wohnhaas C, Friedemann K, Busko D, Landfester K, Balushev S, Crespy D, Turshatov A (2013) *ACS Macro Lett* 2:446–450
12. Kang JH, Reichmanis E (2012) *Angew Chem Int Ed* 51:11841–11844
13. Kim J-H, Kim J-H (2015) *ACS Photonics* 2:633–638
14. Kim J-H, Deng F, Castellano FN, Kim J-H (2014) *ACS Photonics* 1:382–388
15. Svagan AJ, Busko D, Avlasevich Y, Glasser G, Balushev S, Landfester K (2014) *ACS Nano* 8:8198–8207
16. Terech P, Weiss RG (1997) *Chem Rev* 97:3133–3160
17. Okesola BO, Vieira VM, Cornwell DJ, Whitelaw NK, Smith DK (2015) *Soft Matter* 11:4768–4787
18. Sripathy K, MacQueen RW, Peterson JR, Cheng YY, Dvořák M, McCamey DR, Treat ND, Stingelin N, Schmidt TW (2015) *J Mater Chem C* 3:616–622
19. Vadrucci R, Weder C, Simon YC (2015) *Mater Horiz* 2:120–124
20. Duan P, Yanai N, Nagatomi H, Kimizuka N (2015) *J Am Chem Soc* 137:1887–1894
21. Islangulov RR, Lott J, Weder C, Castellano FN (2007) *J Am Chem Soc* 129:12652–12653
22. Singh-Rachford TN, Lott J, Weder C, Castellano FN (2009) *J Am Chem Soc* 131:12007–12014
23. Kim J-H, Deng F, Castellano FN, Kim J-H (2012) *Chem Mater* 24:2250–2252
24. Monguzzi A, Bianchi F, Bianchi A, Mauri M, Simonutti R, Ruffo R, Tubino R, Meinardi F (2013) *Adv Energy Mater* 3:680–686
25. Merkel PB, Dinnocenzo JP (2009) *J Lumin* 129:303–306
26. Monguzzi A, Tubino R, Meinardi F (2009) *J Phys Chem C* 113(7):1171–1174
27. Lee SH, Lott JR, Simon YC, Weder C (2013) *J Mater Chem C* 1:5142–5148
28. Zimmermann J, Mulet R, Scholes GD, Wellens T, Buchleitner A (2014) *J Chem Phys* 141:184104
29. Monguzzi A, Frigoli M, Larpent C, Tubino R, Meinardi F (2012) *Adv Funct Mater* 22:139–143
30. Lissau JS, Gardner JM, Morandeira A (2011) *J Phys Chem C* 115:23226–23232
31. Lissau JS, Nauroozi D, Santoni M-P, Ott S, Gardner JM, Morandeira A (2013) *J Phys Chem C* 117:14493–14501
32. Lissau JS, Nauroozi D, Santoni M-P, Edvinsson T, Ott S, Gardner JM, Morandeira A (2015) *J Phys Chem C* 119:4550–4564
33. Karpicz R, Puzinas S, Gulbinas V, Vakhnin A, Kadashchuk A, Rand BP (2014) *Chem Phys* 429:57–62
34. Jankus V, Snedden EW, Bright DW, Whittle VL, Williams JAG, Monkman A (2013) *Adv Funct Mater* 23:384–393
35. Vadrucci R, Weder C, Simon YC (2014) *J Mater Chem C* 2:2837
36. Wu TC, Congreve DN, Baldo MA (2015) *Appl Phys Lett* 107:031103
37. Lee SH, Ayer MA, Vadrucci R, Weder C, Simon YC (2014) *Polym Chem* 5:6898–6904
38. Mahato P, Monguzzi A, Yanai N, Yamada T, Kimizuka N (2015) *Nat Mater* 14:924–930
39. Duan P, Yanai N, Kurashige Y, Kimizuka N (2015) *Angew Chem Int Ed* 54:7544–7549
40. Lee S-H, Sonseca Á, Vadrucci R, Giménez E, Foster EJ, Simon YC (2014) *J Inorg Organomet Polym* 24:898–903
41. MacQueen RW, Schulze TF, Khoury T, Cheng YY, Stannowski B, Lips K, Crossley MJ, Schmidt T (2013) *Proc SPIE* 882408
42. Trupke T, Green MA, Würfel P (2002) *J Appl Phys* 92:4117



43. Atre AC, Dionne JA (2011) *J Appl Phys* 110:034505–034505–034505–034509
44. de Wild J, Meijerink A, Rath JK, van Sark WGJHM, Schropp REI (2011) *Energy Environ. Sci.* 4:4835
45. Gray V, Dzebo D, Abrahamsson M, Albinsson B, Moth-Poulsen K (2014) *Phys Chem Chem Phys* 16:10345–10352
46. Schulze TF, Schmidt TW (2015) *Energy Environ Sci* 8:103–125
47. Goldschmidt JC, Fischer S (2015) *Adv Opt Mater* 3:510–535
48. Schulze TF, Czolk J, Cheng Y-Y, Fückel B, MacQueen RW, Khoury T, Crossley MJ, Stannowski B, Lips K, Lemmer U, Colsmann A, Schmidt TW (2012) *J Phys Chem C* 116:22794–22801
49. Cheng YY, Fückel B, MacQueen RW, Khoury T, Clady RGCR, Schulze TF, Ekins-Daukes NJ, Crossley MJ, Stannowski B, Lips K, Schmidt TW (2012) *Energy Environ Sci* 5:6953
50. Schulze TF, Cheng YY, Fückel B, MacQueen RW, Danos A, Davis NJLK, Tayebjee MJY, Khoury T, Clady RGCR, Ekins-Daukes NJ, Crossley MJ, Stannowski B, Lips K, Schmidt TW (2012) *Aust J Chem* 65:480
51. Nattestad A, Cheng YY, MacQueen RW, Schulze TF, Thompson FW, Mozer AJ, Fückel B, Khoury T, Crossley MJ, Lips K, Wallace GG, Schmidt TW (2013) *J Phys Chem Lett* 4:2073–2078
52. Khnayzer RS, Blumhoff J, Harrington JA, Haefele A, Deng F, Castellano FN (2012) *Chem Commun* 48:209–211
53. Kim JH, Kim JH (2012) *J Am Chem Soc* 134:17478–17481
54. Liu Q, Yang T, Feng W, Li F (2012) *J Am Chem Soc* 134:5390–5397
55. Liu Q, Yin B, Yang T, Yang Y, Shen Z, Yao P, Li F (2013) *J Am Chem Soc* 135:5029–5037
56. Askes SH, Bahreman A, Bonnet S (2014) *Angew. Chem. Int Ed* 53:1029–1033
57. Borisov SM, Larndorfer C, Klimant I (2012) *Adv Funct Mater* 22:4360–4368
58. Mongin C, Garakyaraghi S, Razgoniaeva N, Zamkov M, Castellano FN (2016) *Science* 351:369–372